

PAPER

# Temporal evolution of the Seebeck coefficient in an ac driven strongly correlated quantum dot

To cite this article: A Goker and E Gedik 2013 *J. Phys.: Condens. Matter* **25** 125301

View the [article online](#) for updates and enhancements.

## You may also like

- [Enhancing quantum coherence of a fluxonium qubit by employing flux modulation with tunable-complex-amplitude](#)  
Jia-Ming Cheng, Yong-Chang Zhang, Xiang-Fa Zhou et al.
- [Influence of Modified Collisional Damping on Saturation of Plasma Beat Waves](#)  
Zhong Quande
- [Striations in electronegative capacitive chlorine discharges: effects of pressure, frequency, voltage and secondary electron emission](#)  
Bahram Mahdavi-pour and Jon Tomas Gudmundsson

# Temporal evolution of the Seebeck coefficient in an ac driven strongly correlated quantum dot

A Goker<sup>1</sup> and E Gedik<sup>2</sup>

<sup>1</sup> Department of Physics, Bilecik University, 11210, Gülümbe, Bilecik, Turkey

<sup>2</sup> Department of Physics, Eskisehir Osmangazi University, 26480, Meselik, Eskisehir, Turkey

E-mail: [aihsan.goker@bilecik.edu.tr](mailto:aihsan.goker@bilecik.edu.tr)

Received 5 November 2012, in final form 1 February 2013

Published 19 February 2013

Online at [stacks.iop.org/JPhysCM/25/125301](http://stacks.iop.org/JPhysCM/25/125301)

## Abstract

We study the response of the thermopower of a quantum dot in the Kondo regime to sinusoidal displacement of the dot energy level via a gate voltage using time dependent non-crossing approximation and linear response Onsager relations. Instantaneous thermopower begins to exhibit complex fluctuations when the driving amplitude is increased at constant driving frequency. We also find that the time averaged thermopower decreases steadily until it saturates at constant driving amplitude as a function of inverse driving frequency. On the other hand, time averaged thermopower is found to be quite sensitive to ambient temperature at all driving frequencies for large driving amplitudes. We discuss the underlying microscopic mechanism for these peculiarities based on the behaviour of the dot density of states.

(Some figures may appear in colour only in the online journal)

## 1. Introduction

Single electron transistors consisting of a nanodevice placed between electrodes have received much attention recently since they are believed to carry great promise as a future replacement for the conventional MOSFET, which will reach its limit at 10 nm in 2016 [1]. Unparalleled precision enabled by the nanotechnology revolution brought immense momentum to this field. Determination of the switching behaviour of these devices in the presence of strong electron–electron correlations is a requirement for their utilization in electrical circuits. Moreover, investigation of transient electron dynamics [2] should also help fine tuning of quantum computers [3] as well as single electron guns [4].

Initial investigations on the effect of Kondo correlations on the transient current flowing immediately after abrupt changing of the gate or bias voltage [5–7] uncovered different timescales [8, 9]. Since it takes Kondo resonance a considerable amount of time to become fully formed [5], strong interference between the Kondo resonance and the Van Hove singularities in the contacts' density of states

results in damped oscillations in the long timescale for an asymmetrically coupled system [10]. Better agreement between the experiments and theoretical predictions can be attained by using realistic density of states for the contacts with the help of ab initio methods [11, 12].

Transport experiments can derive additional benefit from the measurement of thermopower (Seebeck coefficient)  $S$ , since its sign is a benchmark providing direct information about the alignment of the impurity orbitals with respect to the Fermi level of the contacts. Consequently, this provides unambiguous evidence about the existence of Kondo resonance at the Fermi level of the contacts. Recent experiments measuring thermoelectricity in molecular junctions yielded key signatures confirming these predictions [13–16].

Previous theoretical studies on this setup mainly focused on the steady-state behaviour of the thermopower. Different groups independently observed that the position of the dot level is critical to determine the sign of the thermopower in the Kondo regime [17, 18]. In the first attempt to study the transient behaviour of thermopower [19], it was uncovered that the inverse of the saturated decay time of thermopower to its steady-state value is equal to the Kondo temperature

when the dot level is abruptly moved to a position close to the Fermi level such that the Kondo resonance is present in the final position.

It is quite interesting to investigate the effect of changing the left and right tunnel couplings of the dot to the electrodes sinusoidally with a phase lag [20]. If the phase lag is nonzero, this results in asymmetrical coupling. Another interesting situation arises when the dot energy level is subjected to time dependent ac perturbations in symmetrical coupling. This enables us to monitor the evolution of thermopower in real time when the Kondo temperature changes constantly as a result of the oscillatory motion of the dot energy level between the leads [21, 22]. This type of Kondo shuttling has been made possible with experimental advances on controlling dot–lead coupling [23, 24]. We previously studied the behaviour of current in this setup and found that the time averaged conductance exhibits considerable deviation from its monotonic decrease as a function of applied bias when the bias is equal to the driving frequency [25]. It is our aim in this paper to study both the instantaneous and time averaged values of the thermopower when the dot level is driven sinusoidally by means of a gate voltage.

## 2. Theory

The physical setup of a single electron transistor consists of a single discrete degenerate energy level  $\epsilon_{\text{dot}}$  coupled to continuum electrons in the electrodes. This is a quantum impurity problem and it can be represented by the Anderson Hamiltonian

$$H(t) = \sum_{\sigma} \epsilon_{\text{dot}}(t)n_{\sigma} + \sum_{k\alpha\sigma} \epsilon_k n_{k\alpha\sigma} + \frac{1}{2} \sum U_{\sigma,\sigma'} n_{\sigma} n_{\sigma'} + \sum_{k\alpha\sigma} [V_{\alpha}(\epsilon_{k\alpha}, t)c_{k\alpha\sigma}^{\dagger}c_{\sigma} + \text{H.c.}], \quad (1)$$

adequately, where  $c_{\sigma}^{\dagger}$  ( $c_{\sigma}$ ) and  $c_{k\alpha\sigma}^{\dagger}$  ( $c_{k\alpha\sigma}$ ) with  $\alpha = \text{L, R}$  create (annihilate) an electron of spin  $\sigma$  in the dot energy level and in the left (L) and right (R) electrodes respectively. The  $n_{\sigma}$  and  $n_{k\alpha\sigma}$  are the number operators for the dot level and the electrode  $\alpha$ .  $V_{\alpha}$  are the tunnelling amplitudes between the electrode  $\alpha$  and the quantum dot. The Coulomb repulsion energy  $U$  is assumed to be infinity, hence the occupation of the dot level is strictly restricted to unity. In this paper, we will adopt atomic units where  $\hbar = k_{\text{B}} = e = 1$ .

In our procedure, we perform slave boson transformation for the Anderson Hamiltonian. The electron operators on the dot are rewritten in terms of a massless (slave) boson operator and a pseudofermion operator as

$$c_{\sigma} = b^{\dagger}f_{\sigma}, \quad (2)$$

subject to the requirement that

$$Q = b^{\dagger}b + \sum_{\sigma} f_{\sigma}^{\dagger}f_{\sigma} = 1. \quad (3)$$

The last requirement is essentially a bookkeeping tool that prevents the double occupancy in the original Hamiltonian when  $U \rightarrow \infty$ . The main advantage of using this

transformation is that we can now safely drop the quartic Hubbard term since its effects are now incorporated in other terms anyway. The transformed Hamiltonian then becomes

$$H(t) = \sum_{\sigma} \epsilon_{\text{dot}}(t)n_{\sigma} + \sum_{k\alpha\sigma} \left[ \epsilon_k n_{k\alpha\sigma} + V_{\alpha}(\epsilon_{k\alpha}, t)c_{k\alpha\sigma}^{\dagger}b^{\dagger}f_{\sigma} + \text{H.c.} \right], \quad (4)$$

where  $f_{\sigma}^{\dagger}$  ( $f_{\sigma}$ ) and  $b^{\dagger}$  ( $b$ ) with  $\alpha = \text{L, R}$  create (annihilate) an electron of spin  $\sigma$  and a slave boson on the dot respectively.

Assuming no explicit time dependency for the hopping matrix elements, the coupling of the quantum dot to the electrodes for a symmetrically coupled system can be expressed as  $\Gamma(\epsilon) = \bar{\Gamma}\rho(\epsilon)$ , where  $\bar{\Gamma}$  is a constant given by  $\bar{\Gamma} = 2\pi|V(\epsilon_f)|^2$  and  $\rho(\epsilon)$  is the density of states function of the electrodes.

The retarded Green function can now be rewritten in terms of the slave boson and pseudofermion Green functions [10] as

$$G^R(t, t_1) = -i\theta(t - t_1)[G_{\text{pseudo}}^R(t, t_1)B^<(t_1, t) + G_{\text{pseudo}}^<(t, t_1)B^R(t_1, t)]. \quad (5)$$

It is a quite cumbersome and highly nontrivial task to compute the values of these double time Green functions in real time, as the dot level is in constant motion. We accomplish this by solving coupled integro-differential Dyson equations in a two-dimensional Cartesian grid. However, the self-energy of the pseudofermion and slave boson must be built into these equations in order to be able to obtain a solution. To this end, we invoke the non-crossing approximation (NCA) to express the pseudofermion and slave boson self-energies [26, 9]. As the name implies, the NCA ignores higher order corrections where propagators cross each other. Consequently, it provides erroneous results in finite magnetic fields and when the ambient temperature is an order of magnitude smaller than the Kondo energy scale. We will avoid these cases in this paper. The main advantage of the NCA is that it is known to give accurate results for dynamical quantities. Upon solving the Dyson equations properly, their values are stored in a square matrix which is translated one step at a time in a diagonal direction.

In linear response, the conductance of the device is given by

$$G(t) = \frac{L_{11}(t)}{T}, \quad (6)$$

and the Seebeck coefficient or the thermopower is expressed as

$$S(t) = \frac{L_{12}(t)}{TL_{11}(t)}, \quad (7)$$

where the Onsager coefficients are

$$L_{11}(t) = T\text{Im} \left( \int_{-\infty}^t dt_1 \int \frac{d\epsilon}{2\pi} e^{i\epsilon(t-t_1)} \Gamma(\epsilon) \times G^r(t, t_1) \frac{\partial f(\epsilon)}{\partial \epsilon} \right) \quad (8)$$

and

$$L_{12}(t) = T^2 \text{Im} \left( \int_{-\infty}^t dt_1 \int \frac{d\epsilon}{2\pi} e^{i\epsilon(t-t_1)} \Gamma(\epsilon) \times G^r(t, t_1) \frac{\partial f(\epsilon)}{\partial T} \right). \quad (9)$$

where  $f(\epsilon) = \frac{1}{1+e^{\beta\epsilon}}$  is the Fermi–Dirac distribution with  $\beta = \frac{1}{T}$ .

Instantaneous conductance exhibits oscillations between zero, occurring at the lowest position of the dot level, and a maximum, taking place at its closest location to the Fermi level. We previously analysed the conductance for this setup in detail [25] and presented the time averaged density of states for the dot as well.

### 3. Results and discussion

In this work, we will investigate the behaviour of equation (7) for a quantum dot in the Kondo regime whose energy level is driven sinusoidally via a gate voltage. We will report our results in atomic units; therefore, one needs to multiply our thermopower values by  $k_B/e$  to obtain the SI value in terms of volts per kelvin. This conversion factor turns out to be  $0.86 \times 10^{-4}$ . This sinusoidal motion results in periodic modulations of the main Kondo resonance and its satellites. Time averaged thermopower has been previously studied in this system neglecting the Kondo effect [27]. We would like to make this model more realistic by including the Kondo effect in this analysis, since strong electron correlation effects play a crucial role in confined nanostructures like quantum dots. We will only consider the linear response instantaneous thermopower due to the validity of Onsager relations in this regime.

The Kondo effect has long been a trademark of many body physics taking place at sufficiently low temperatures due to a hybridization between the net spin localized inside an impurity and the continuum electrons of a nearby metal. Its main manifestation is a sharp resonance around the Fermi level of the metal arising when the impurity level is located below the Fermi level. The linewidth of this Kondo resonance is roughly equal to a low energy scale called the Kondo temperature, which is denoted by  $T_K$  and expressed as

$$T_K \approx \left( \frac{D\Gamma}{4} \right)^{\frac{1}{2}} \exp \left( -\frac{\pi|\epsilon_{\text{dot}}|}{\Gamma} \right). \quad (10)$$

In equation (10)  $D$  is the half-bandwidth of the conduction electrons, while  $\Gamma = \bar{\Gamma}\rho(\epsilon_f)$ .

We will first consider the behaviour of the instantaneous value of the thermopower when the dot energy level is modulated sinusoidally via a gate voltage. We can represent the instantaneous behaviour of the dot level as

$$\epsilon_{\text{dot}}(t) = -5\Gamma - A \cos(\Omega t), \quad (11)$$

where  $A$  is the driving amplitude and  $\Omega$  is the driving frequency. The dc value of the dot energy level was chosen as  $-5\Gamma$  to ensure that the dot level lies sufficiently below the

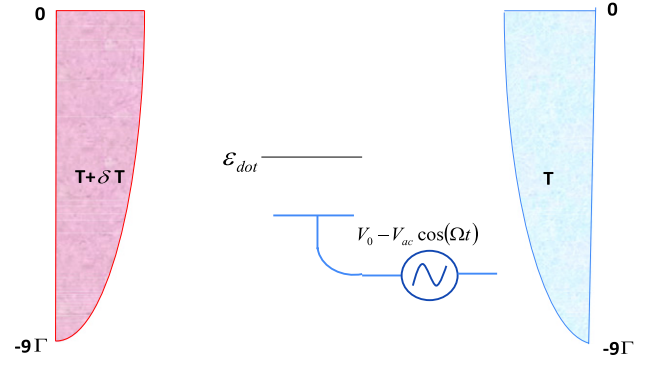


**Figure 1.** The density of states of both contacts alongside the application of an ac gate voltage to the dot energy level as well as the temperature gradient between the contacts.

Fermi level such that the Kondo temperature is much lower than the ambient temperature. In principle, it is possible to choose a lower dot energy level as the dc value. However, it would be problematic with our parameters, because we would need to increase the driving amplitudes even higher in that case to approach the Fermi level sufficiently, and the dot energy level would go beyond the bandwidth, which is at  $-9\Gamma$  in its lowest position. This type of modulation induces a continuous change in Kondo temperature  $T_K$  since its value depends on the dot energy level in equation (10). Consequently, the shape of the Kondo resonance pinned to the Fermi level of the contacts constantly changes. The parabolic structure of the density of states of the contacts and the temperature gradient applied to them is depicted schematically in figure 1 alongside the application of gate voltage to the dot energy level.

Instantaneous thermopower is shown in figure 2 for three different driving amplitudes  $A$  immediately after the gate voltage has been turned on at constant driving frequency and ambient temperature. Since the dot level is oscillating sinusoidally, the value of the Kondo temperature is fluctuating alongside it between zero and a maximum value. These maximum values are  $T_K = 0.0022\Gamma$ ,  $T_K = 0.00055\Gamma$  and  $T_K = 0.00011\Gamma$  for driving amplitudes of  $3\Gamma$ ,  $2.5\Gamma$  and  $2\Gamma$  respectively. In this figure, thermopower slowly acquires a positive value as the dot level approaches the Fermi level for all driving amplitudes. For the smallest driving amplitude, it reaches a maximum positive value at its closest point to the Fermi level before it starts decreasing again as the dot level begins to go down.

However, this smooth behaviour changes abruptly when we start increasing the driving amplitude. When the driving amplitude becomes  $2.5\Gamma$ , the value of the instantaneous thermopower initially acquires a positive value as in the previous case; however, it suddenly starts to decrease as the dot level approaches the Fermi level and dips into negative territory before it rebounds and increases again as the dot level gets away from the Fermi level. When the driving amplitude is increased even further, instantaneous thermopower starts decreasing earlier, and more importantly it dips deeper into negative territory before it rebounds as the dot level is pushed back. This fluctuating behaviour is repeated over many cycles

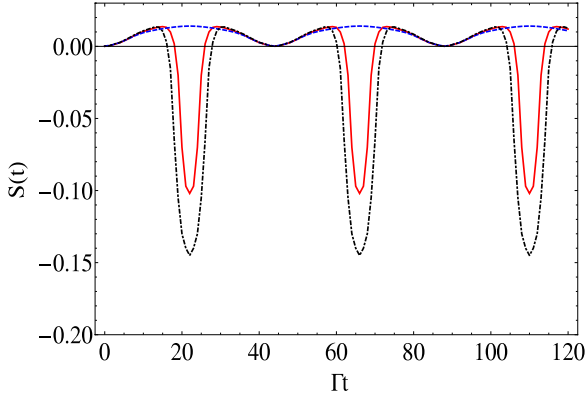


**Figure 2.** The instantaneous thermopower  $S(t)$  immediately after the gate voltage has been turned on for driving amplitudes of  $2.0\Gamma$  (blue dashed),  $2.5\Gamma$  (red solid) and  $3.0\Gamma$  (black dot-dashed) at  $T = 0.003\Gamma$  and  $\Omega = 0.14\Gamma$  in linear response.

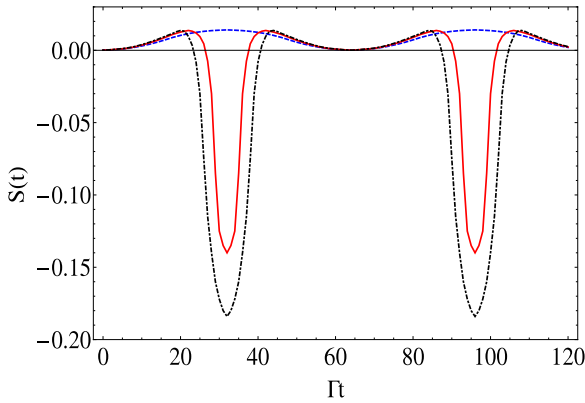


**Figure 3.** The instantaneous thermopower  $S(t)$  immediately after the gate voltage has been turned on for driving amplitudes of  $2.0\Gamma$  (blue dashed),  $2.5\Gamma$  (red solid) and  $3.0\Gamma$  (black dot-dashed) at  $T = 0.003\Gamma$  and  $\Omega = 0.10\Gamma$  in linear response.

since the dot level's motion follows the gate voltage and is consequently strictly sinusoidal.

Figure 3 shows the instantaneous thermopower for the same parameters as used in figure 2, but the gate voltage is applied with a smaller frequency this time. An obvious consequence of this for the instantaneous thermopower is the longer oscillation periods for all driving amplitudes. Besides this trivial effect, we notice that the smooth oscillation behaviour for the smallest driving amplitude did not change much. On the other hand, there are significant changes for the other two larger driving amplitude cases compared with the larger driving frequency. Their fluctuation behaviour seems qualitatively similar, but they both dive much deeper into negative territory as the dot level comes close to the Fermi level. This effect is quite pronounced for both cases.

Having observed these peculiarities, one would be naturally inclined to find out whether these conclusions are valid for other driving frequencies and ambient temperatures. In order to pinpoint this issue, we calculated the time averaged value of the instantaneous thermopower over a full period for two different ambient temperatures at several different driving frequencies. Time averaged thermopower for the

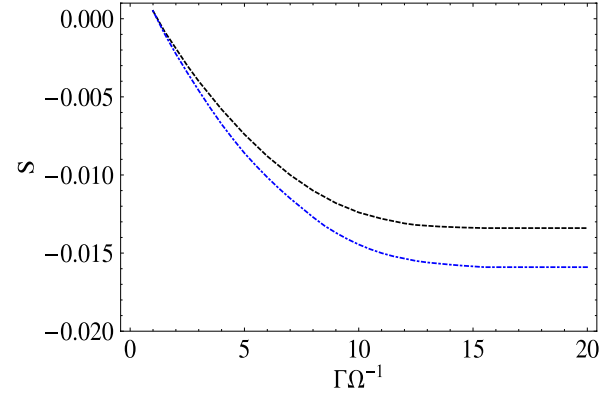


**Figure 4.** The value of the thermopower averaged over a period as a function of inverse driving frequency at  $T = 0.003\Gamma$  (black dashed) and  $T = 0.002\Gamma$  (blue dot-dashed) for a driving amplitude of  $2.5\Gamma$ .

smallest driving amplitude was not sensitive to the changes in temperature so we are not reporting it in the following. We will elucidate the reason for this later.

Figure 4 depicts the time averaged value of the instantaneous thermopower as a function of inverse driving frequency for two different ambient temperatures at a constant driving amplitude of  $2.5\Gamma$ . The first conclusion that can be drawn from this figure is that the absolute value of the time averaged thermopower is always different at all driving frequencies when the ambient temperature changes. Moreover, the absolute value of the time averaged thermopower starts to increase for both ambient temperatures as the driving frequency is decreased, but it saturates at a certain driving frequency and stays constant thereafter.

This is a quite peculiar and interesting observation, and in order to test whether it is valid for other driving amplitudes as well we performed the same analysis for the largest driving amplitude of  $3.0\Gamma$ , keeping all the other parameters constant. We do not increase the driving amplitude beyond this value to avoid entering the mixed valence regime where the Kondo and Breit-Wigner resonances overlap. We are only interested in investigating the effect of Kondo resonance on thermopower in this paper. The result for this driving amplitude can be seen in figure 5. It is clear from this figure that the conclusion we had drawn is indeed valid here too. Namely, time averaged thermopower is quite sensitive to ambient temperature and it saturates when the driving frequency is decreased. However, there is an important difference. Absolute values of the time averaged thermopower at both ambient temperatures and all driving frequencies are greater than the previous case in figure 4 where the driving amplitude was  $2.5\Gamma$ . This is also an important result which we will dwell on below.

We now want to provide an unambiguous microscopic explanation for the results we presented above. It is clear that the development of the Kondo resonance plays a crucial role in transport of this prototypical device. Evolution of the Kondo resonance is incorporated in the dot density of states, and the relation between the dot density of states and the thermopower at low temperatures is given by the Sommerfeld expansion. It

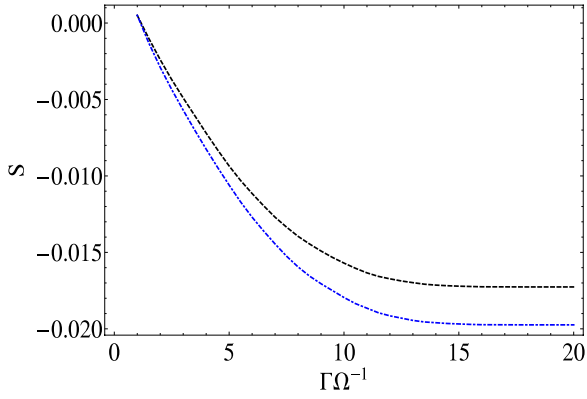


**Figure 5.** The value of the thermopower averaged over a period as a function of inverse driving frequency at  $T = 0.003\Gamma$  (black dashed) and  $T = 0.002\Gamma$  (blue dot-dashed) for a driving amplitude of  $3.0\Gamma$ .

can be expressed as

$$S(T) = -\frac{\pi^2 T}{3 A(0, T)} \left. \frac{\partial A}{\partial \epsilon} \right|_{\epsilon=0} \quad (12)$$

in atomic units. In this equation,  $A(0, T)$  is the value of the dot density of states at the Fermi level of the contacts and  $\frac{\partial A}{\partial \epsilon}$  is its derivative. It has been shown that the formation of the Kondo resonance occurs slightly above the Fermi level [28], making the derivative of the dot density of states at Fermi level positive at ambient temperatures close to or less than the Kondo temperature. This will give rise to a negative thermopower in this regime. On the other hand, Breit–Wigner resonance around the dot energy level is the only prominent feature of the dot density of states in the absence of Kondo resonance at ambient temperatures much greater than the Kondo temperature. Consequently, the thermopower will be positive if the dot level is positioned sufficiently away from the Fermi level, since the dot density of states at Fermi level will lie in the long tail of the Breit–Wigner resonance. Thus, a shift in the sign of the thermopower by tuning the temperature is a signature of the emergence of the Kondo resonance.

When the driving amplitude is  $2.0\Gamma$ , the dot level cannot approach the Fermi level to be able to develop the Kondo resonance. Therefore,  $T \gg T_K$  for all dot levels involved in this oscillation, and the thermopower never dips into negative territory. It starts from zero when the dot level is farthest from the Fermi level because the density of states is essentially zero everywhere around the Fermi level. However, it gradually acquires a positive value as the dot level approaches the Fermi level because the tail of the Breit–Wigner resonance starts to reach the Fermi level, causing a negative slope there. Thermopower reaches a maximum positive value before the dot level starts to retreat. The values are not sensitive to temperature because Kondo resonance cannot be formed at all at any stage of this motion.

The oscillation of the dot energy level covers a larger energy range as the driving amplitude is ramped up to  $2.5\Gamma$ . The value of the thermopower initially follows the value obtained when the driving amplitude was  $2.0\Gamma$ , but it starts to deviate significantly when the dot level approaches the Fermi

level because the Kondo resonance begins to emerge there. This is accompanied by a change in slope of the density of states of the dot and consequently a change in sign of the thermopower. The thermopower sees its minimum value when the dot level is at its closest point to the Fermi level because the Kondo resonance is at its most developed form here. As the dot level starts to retreat, the Kondo resonance is gradually suppressed, hence the thermopower becomes positive after a while.

Similar conclusions hold for the largest driving amplitude of  $3.0\Gamma$  except for the fact that the instantaneous thermopower dips lower into negative territory since the dot energy level manages to get even closer to the Fermi level, hence the Kondo resonance is more developed.

The saturation behaviour of the time averaged thermopower at low driving frequencies is also closely related to the development of the Kondo resonance. As the driving frequency is lowered, the dot energy level begins to spend more time near the Fermi level. This in turn gives the Kondo resonance more time to develop, since its full formation takes a considerable amount of time [5]. Consequently, time averaged thermopower values start to increase in negative territory. However, when the driving frequency is lowered below a certain value, we observe that the time averaged thermopower saturates. This is simply because the dot level spends sufficient time in the vicinity of the Fermi level to enable the full development of the Kondo resonance.

The dependence of the time averaged thermopower curves on ambient temperature is quite interesting too and requires further elaboration. It is clear from both figures 4 and 5 that the difference between the time averaged values obtained at the same driving frequency increases as the driving frequency is reduced, until it stays constant below a certain frequency. This behaviour is further testimony to the crucial role that development of the Kondo resonance plays in thermopower. At elevated driving frequencies, time averaged thermopower is not sensitive to ambient temperature because the dot level cannot spend sufficient time near the Fermi level. Naturally, the Kondo resonance cannot be formed adequately, hence a lack of sensitivity to ambient temperature. As the driving frequency is reduced, the difference becomes more pronounced and stays constant after the Kondo resonance gets the chance to develop itself fully below a certain frequency.

## 4. Conclusion

In conclusion, we studied in linear response both the instantaneous and time averaged values of thermopower for a quantum dot sinusoidally driven by a gate voltage. We found that the instantaneous thermopower exhibits complex fluctuations as the driving amplitude is ramped up. We interpreted the origin of dipping into negative territory as a sign of development of the Kondo resonance at Fermi level. We studied the behaviour of the time averaged thermopower as a function of inverse driving frequency and observed that it tends to saturate at low driving frequencies. Moreover, the results depend on ambient temperature quite sensitively. We believe that the scenario we discussed in this paper has

great potential to be realized experimentally. The temperature gradient between the contacts can be achieved with laser irradiation, and the sinusoidal motion of the dot level can easily be realized with an ac gate voltage. We also think that state of the art ultrafast pump–probe techniques [29, 30] could make recording thermopower in real time possible. Therefore, we hope to create motivation and experimental progress in this field with our novel results.

## Acknowledgments

The authors thank TÜBİTAK for generous financial support via grant 111T303.

## References

- [1] Likharev K K 2003 *Nano and Giga Challenges in Microelectronics* ed J Greer, A Korkin and J Labanowski (Dordrecht: Elsevier) pp 27–68
- [2] Lu W, Ji Z, Pfeiffer L, West K W and Rimberg A J 2003 *Nature* **423** 422
- [3] Elzerman J M, Hanson R, van Beveren L H W, Witkamp B, Vandersypen L M K and Kouwenhoven L P 2004 *Nature* **430** 431
- [4] Fève G, Mahe A, Berroir J M, Kontos T, Placais B, Glatli D C, Cavanna A, Etienne B and Jin Y 2007 *Science* **316** 1169
- [5] Nordlander P, Pustilnik M, Meir Y, Wingreen N S and Langreth D C 1999 *Phys. Rev. Lett.* **83** 808–11
- [6] Plihal M, Langreth D C and Nordlander P 2000 *Phys. Rev. B* **61** R13341
- [7] Merino J and Marston J B 2004 *Phys. Rev. B* **69** 115304
- [8] Plihal M, Langreth D C and Nordlander P 2005 *Phys. Rev. B* **71** 165321
- [9] Izmaylov A F, Goker A, Friedman B A and Nordlander P 2006 *J. Phys.: Condens. Matter* **18** 8995
- [10] Goker A, Friedman B A and Nordlander P 2007 *J. Phys.: Condens. Matter* **19** 376206
- [11] Goker A, Zhu Z Y, Manchon A and Schwingenschlogl U 2010 *Phys. Rev. B* **82** 161304
- [12] Goker A, Zhu Z Y, Manchon A and Schwingenschlogl U 2011 *Chem. Phys. Lett.* **509** 48
- [13] Reddy P, Jang S Y, Segalman R A and Majumdar A 2007 *Science* **315** 1568
- [14] Baheti K, Malen J A, Doak P, Reddy P, Jang S Y, Tilley T D, Majumdar A and Segalman R A 2008 *Nano Lett.* **8** 715
- [15] Malen J A, Doak P, Baheti K, Tilley T D, Majumdar A and Segalman R A 2009 *Nano Lett.* **9** 3406
- [16] Tan A, Sadat S and Reddy P 2010 *Appl. Phys. Lett.* **96** 13110
- [17] Dong B and Lei X L 2002 *J. Phys.: Condens. Matter* **14** 11747
- [18] Costi T A and Zlatic V 2010 *Phys. Rev. B* **81** 235127
- [19] Goker A and Uyanik B 2012 *Phys. Lett. A* **376** 2735
- [20] Arrachea L, Yeyati A L and Martin-Rodero A 2008 *Phys. Rev. B* **77** 165326
- [21] Al-Hassanieh K A, Busser C A, Martins G B and Dagotto E 2005 *Phys. Rev. Lett.* **95** 256807
- [22] Kiselev M N, Kikoin K, Shekhter R I and Vinokur V M 2006 *Phys. Rev. B* **74** 233403
- [23] Scheible D V, Weiss C, Kotthaus J P and Blick R H 2004 *Phys. Rev. Lett.* **93** 186801
- [24] Parks J J, Champagne A R, Hutchison G R, Flores-Torres S, Abruna H D and Ralph D C 2007 *Phys. Rev. Lett.* **99** 026601
- [25] Goker A 2008 *Solid State Commun.* **148** 230
- [26] Shao H X, Langreth D C and Nordlander P 1994 *Phys. Rev. B* **49** 13929
- [27] Chi F and Dubi Y 2012 *J. Phys.: Condens. Matter* **24** 145301
- [28] Costi T A, Hewson A C and Zlatic V 1994 *J. Phys.: Condens. Matter* **6** 2519
- [29] Terada Y, Yoshida S, Takeuchi O and Shigekawa H 2010 *J. Phys.: Condens. Matter* **22** 264008
- [30] Terada Y, Yoshida S, Takeuchi O and Shigekawa H 2010 *Nature Photon.* **4** 869